PHYSICAL REVIEW B **79**, 165210 (2009)

Identification of two hydrogen donors in ZnO

E. V. Lavrov,* F. Herklotz, and J. Weber
Technische Universität Dresden, 01062 Dresden, Germany
(Received 13 February 2009; published 28 April 2009)

A combined study of Raman scattering, IR absorption, photoluminescence, and photoconductivity was performed in ZnO. Two shallow donors—hydrogen at the bond-centered lattice site, H_{BC}, and hydrogen bound in an oxygen vacancy, H_O—were identified. Donor H_{BC} has an ionization energy of 53 meV. The recombination of an exciton bound to H_{BC} gives rise to the 3360.1 ± 0.2 meV photoluminescence line. A $1s \rightarrow 2p$ donor transition at 330 cm^{-1} is detected in the Raman scattering and photoconductivity spectra. The stretch mode of the associated O-H bond is detected in IR absorption at 3611 cm^{-1} with an effective charge of $(0.28 \pm 0.03)e$. The concentration of H_{BC} was determined from the frequency shift of the E_1(LO) phonon-plasmon mode at 591 cm^{-1}. The H_O donor in ZnO [A. Janotti and C. G. Van de Walle, Nat. Mater. **6**, 44 (2007)] has an ionization energy of 47 meV. The excitonic recombination at H_O leads to the previously labeled I_4 line at 3362.8 meV. Photoconductivity spectra reveal the $1s \rightarrow 2p$ donor transition at 265 cm^{-1}.

DOI: 10.1103/PhysRevB.79.165210 PACS number(s): 61.72.uj, 63.20.Pw, 71.55.Gs, 78.30.Fs

I. INTRODUCTION

In the 1950s, Mollwo[1] and Thomas and Lander[2] detected *n*-type conductivity after introducing hydrogen into ZnO at elevated temperatures. Since then, the influence of hydrogen on doping and defect passivation in ZnO is an object of active research.

Three types of hydrogen-related defects are discussed in the literature. These are (i) hydrogen-related donors, (ii) acceptor-hydrogen complexes, and (iii) hydrogen molecules H_2. The latter is suggested to be the main reservoir for the so-called "hidden" hydrogen in ZnO, which is not detected by IR spectroscopy but could be converted into a shallow donor in the course of sample processing.[3] No direct experimental evidences for the existence of H_2 have been presented so far.

Contrary to H_2, the detailed spectroscopic features of many acceptor-hydrogen complexes were studied and contributed to our understanding of the microscopic structure of these complexes.[4–10] Hydrogen donors are the topic of the current study. In particular, the properties of the most fundamental species, isolated bond-centered hydrogen, H_{BC}, are discussed.

First-principles investigations carried out by Van de Walle and co-worker[11,12] revealed that isolated hydrogen and hydrogen trapped within the O vacancy, H_O, act as shallow donors in ZnO, and might be responsible for the natural *n*-type conductivity of this material.

Several experimental studies including muon spin rotation,[13,14] electron paramagnetic resonance,[15] photoluminescence (PL),[16] IR absorption,[5,17] Hall-effect measurements,[18] and photoconductivity[19] demonstrated the existence of several hydrogen induced shallow donor states in ZnO.

Previous IR absorption studies revealed two possible hydrogen donors. The one labeled H-I was tentatively identified as a hydrogen bond-centered along the *c* axis.[5] At 10 K the defect results in the absorption line at 3611 cm^{-1} originating from the stretch local vibrational mode (LVM) of the O-H bond. The second donor was assigned to hydrogen located perpendicular to the *c* axis at the antibonding site of the ZnO lattice, H_{AB}.[17] Its LVM frequency at 10 K was found to be 3326 cm^{-1}. The identification of the shallow donors was, however, tentative.

Recent experiments on hydrogen motion in ZnO as well as first-principles calculations rule out H_{AB} as a model for the 3326 cm^{-1} line.[20,21] Instead, a negatively charged Zn vacancy passivated by a single hydrogen atom, $V_{Zn}H^-$,[20] or a calcium-hydrogen complex was suggested.[21] In addition, experiments and theoretical studies have shown that isolated hydrogen is not stable at room temperature (RT) and thus, cannot account for the native *n*-type conductivity of ZnO.[22–24]

In PL studies a line at 3362.8 meV labeled I_4 was detected and identified as a recombination of an exciton bound to a hydrogen donor.[16,25] This signal anneals out at around 500 °C. Based on the thermal stability the donor was tentatively identified with H_O.[12] No additional experimental evidence have been presented in support of this assignment.

In this paper the results of a combined Raman scattering, IR absorption, photoluminescence, and photoconductivity study on two hydrogen shallow donors in ZnO are presented. We identify H_{BC} as the dominant shallow donor which appears immediately after hydrogenation. In addition, the spectroscopic features of H_O are studied in detail.

II. EXPERIMENTAL PROCEDURE

A. Sample preparation

The ZnO crystals used in this work were hexagonal prisms with a diameter of about 2 mm and a length of ~20 mm. The nominally undoped *n*-type single crystals with resistivity of 10–100 Ω cm were grown from the vapor phase at the Institute for Applied Physics, University of Erlangen (Germany).[26,27]

Hydrogen and/or deuterium was introduced into the samples from a remote dc plasma or via annealing in a sealed quartz ampoule. In the case of the dc plasma, the exposure time was 1 h. The sample temperature during the treatment was held at 350 °C. A detailed description of our plasma system is given elsewhere.[5]

The plasma treatment results in a strongly nonuniform concentration profile with more hydrogen located in the near surface layer of the sample. This, however, was not suitable for our Raman measurements, where the 532 nm laser line probes the bulk of ZnO samples. A uniform distribution of hydrogen was achieved by thermal treatments in sealed quartz ampoules filled with hydrogen and/or deuterium gas (pressure of 0.5 bar at room temperature). The thermal treatments were performed in the temperature range of 695–765 °C for 1 h and were terminated by quenching to room temperature in water.

The thermal stability of hydrogen donors was determined from a series of isochronal treatments (anneals) at temperatures from 50 to 290 °C. Each anneal had a duration of 30 min and was carried out in an argon atmosphere. Spectra were recorded after each temperature step.

Uniaxial stress was applied to a sample which was cut with the dimensions of $3.8\times1.9\times1.1$ mm^3, and with axes parallel to $[10\bar{1}0]$, $[1\bar{2}10]$, and c, respectively. The stress was applied parallel to $[10\bar{1}0]$.

Etching of the ZnO samples at RT in orthophosphoric acid allows determining of the spatial distribution of hydrogen donors. Samples with a typical length of 1 cm were gradually immersed into the acid with constant speed. The resulting width of the sample was changed linearly with height: with the maximum (d_{max}) and minimum thickness (d_{min}) on the top and the bottom of the sample, respectively. The difference in width $\Delta=d_{max}-d_{min}$ was in the range of 2–30 μm. Photoluminescence spectra were recorded with the excitation laser spot focused at different heights of the sample. The spot size was less than 50 μm.

B. Raman scattering

Raman measurements were performed in a 90° geometry using the frequency doubled 532 nm line of a Nd:YVO_4 laser for excitation. The scattered light was analyzed using a single grating spectrometer and a cooled Si charge-coupled device detector array. Spectral resolution was 5 cm^{-1}. The measurements were performed with the sample mounted in a cold finger cryostat using liquid helium for cooling. The temperature of the bulk sample was varied by an electrical heater. The actual temperature (T_{act}) within the laser excitation volume was determined from the Stokes to anti-Stokes ratio of the optical phonons of ZnO. It was possible to determine correctly temperatures down to approximately 60 K. For lower temperatures the anti-Stokes intensity was too low to be detected within a reasonable measurement time. For T below 60 K, the temperature was obtained by extrapolation of the experimental dependence of T_{bulk} vs T_{act}.

The scattering geometry is defined with respect to the c axis of the ZnO sample. The x, y, and z axes are parallel to the crystallographic orientations $[10\bar{1}0]$, $[1\bar{2}10]$, and c, respectively. In the notation $a(b,c)d$, $a(d)$ refers to the propagation vector of the incident (scattered) light, whereas $b(c)$ characterizes the polarization vector of the incident (scattered) light. The notation $a(b,-)d$ implies that the scattered light is measured without polarizer.

C. IR absorption

The infrared-absorption spectra were recorded with a BOMEM DA3.01 Fourier transform spectrometer equipped with a globar light source, a KBr beam splitter, and a liquid-nitrogen-cooled InSb detector. The spectral resolution was 0.25–0.5 cm^{-1}. Uniaxial stress was applied to the samples in a home-built stress rig mounted in a He exchange-gas cryostat equipped with ZnSe windows. The stress was supplied by a pneumatic cylinder and transferred via a push rod to the sample. The measurements were performed at 6 K. Polarized light was produced by a wire-grid polarizer with a KRS-5 substrate. More details about Fourier transform infrared setup, and the uniaxial stress rig can be found elsewhere.[28]

D. Photoluminescence

For PL measurements the samples were immersed in liquid He (4.2 K) and excited by the 325 nm line of a HeCd laser with a typical excitation power of 2 mW. The emitted light was dispersed by a $f=1$ m single grating monochromator equipped with a 1200 rules/mm grating and detected by Peltier-cooled photomultiplier (RCA C31034). The spectral resolution was 0.025 nm. The monochromator was calibrated against the lines of a Hg lamp. Spectra were converted from wavelength to energy units taking into account the refractive index of air.[29]

E. Photoconductivity

For photoconductivity measurements the ZnO samples were first etched with orthophosphoric acid for 1 min at room temperature. This procedure thins each side of the sample by 0.6 ± 0.1 μm. Ohmic contacts with an area of 2×2 mm^2 were generated by scratching a mixture of an In-Ga alloy onto the sample surface. The contacts were approximately 1 cm apart and were located on the illuminated face of the sample.

Photoconductivity spectra were recorded with a BOMEM DA3.01 Fourier transform spectrometer equipped with a globar light source, and a mylar (3.5 μm thick) beam splitter. With this configuration, the frequency range from 100 to 600 cm^{-1} could be covered. The spectral resolution was 3 cm^{-1}.

The samples were positioned in an exchange-gas cryostat equipped with polypropylene windows. The temperature was stabilized within 0.1 K in the range of 9–30 K. A platinum resistor was used as a thermometer. Polarized light was produced by putting a wire-grid polarizer with a KRS-5 substrate in front of the cryostat.

III. RESULTS

A. Raman scattering

1. General properties

The Raman spectra measured at $T\leq20$ K in the $x(z,-)y$ geometry are shown in Fig. 1. Before hydrogen treatment [spectrum (a)], the well-known lattice phonon lines are observed. The E_1(LO) phonon is of particular interest for

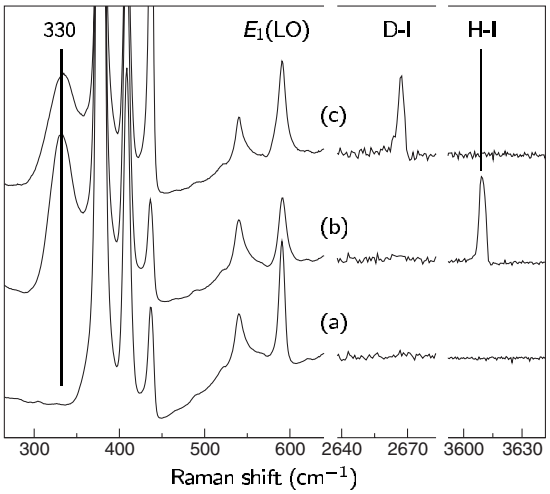

FIG. 1. Sections of Raman spectra obtained on a ZnO sample at $T \leq 20$ K in the $x(z,-)y$ geometry: (a) virgin sample, (b) directly after thermal treatment in the H_2 gas at 725 °C, and (c) the same procedure after replacement of H_2 with D_2.

the current study. The corresponding Raman transition in the virgin sample at helium temperatures is detected at 591 cm^{-1}.[30]

After treatment of the ZnO sample in H_2 gas at 725 °C, two additional features with frequencies at 330 and 3611 cm^{-1} appear in the Raman spectra [spectrum (b) of Fig. 1]. The 3611 cm^{-1} line has been previously observed in IR absorption spectra directly after hydrogen incorporation.[5] This line is a stretch local vibrational mode of an O-H bond. The defect labeled H-I was tentatively assigned to H_{BC}. To the best of our knowledge the Raman line at 330 cm^{-1} has not been reported in the literature.

Spectra of a ZnO sample treated in D_2 gas at 725 °C were also recorded. These are shown as spectrum (c) of Fig. 1. The LVM of the H-I defect shifts downward in frequency by around $\sqrt{2}$ to the value of 2668 cm^{-1}. Note that, to distinguish between hydrogen and deuterium, we label the latter D-I.

Contrary to the stretch mode of H-I, the position of the 330 cm^{-1} signal remains unchanged. Insight into the nature of the 330 cm^{-1} line is obtained from the polarization sensitive Raman spectra presented in Fig. 2. The 330 cm^{-1} signal has the strongest intensity in the $x(z,z)y$ geometry. Note that the nonzero intensity of the 330 cm^{-1} line obtained in other geometries comes mainly from the nonperfect mounting of the sample in the cryostat and the nonideality of the polarizer.

The polarization of the 330 cm^{-1} line implies that the Raman tensor of the corresponding transition is diagonal. Point defects in ZnO show localized modes which belong either to the A_1 or E irreducible representation of the C_{3v} point group. Therefore, only the A_1 mode fulfills the required diagonality.

Hydrogen has also a strong influence on the E_1(LO) phonon mode of ZnO at 591 cm^{-1} (see Fig. 3). The solid line in Fig. 3 shows the spectrum recorded in the $x(z,x)y$ geometry at $T \leq 20$ K from a virgin ZnO sample. The E_1(LO) phonon mode is asymmetric with more intensity located on the low-frequency side of the line.

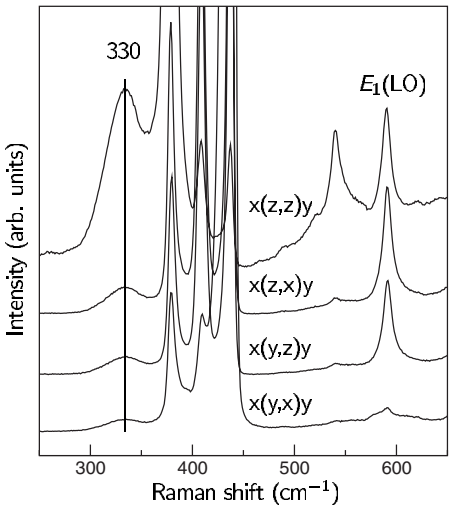

FIG. 2. Polarization sensitive Raman spectra obtained on a ZnO sample treated in H_2 gas at 725 °C. $T \leq 20$ K.

The dashed line in Fig. 3 represents the spectrum obtained on the same sample after thermal treatment in the H_2 gas for 1 h at 725 °C. Obviously, both the intensity of the line and the shape changes: the line becomes weaker and more symmetric. A detailed study of the asymmetric line shape will be presented in the next subsection.

We interpret the effect of hydrogen on the asymmetry with Fano resonance[31] between the E_1(LO) phonon and the continuum of the electronic states in the conduction band. Incorporation of hydrogen enhances the n-type conductivity by the formation of shallow donors. The ionization energies of shallow donors in ZnO are below 73 meV (591 cm^{-1}), which implies that the main condition for the existence of a Fano resonance is fulfilled. Such a behavior is well known in many semiconductors[32] but to the best of our knowledge has not been reported in ZnO so far. The 330 cm^{-1} mode corresponds to a typical $1s \rightarrow 2s$ or $1s \rightarrow 2p_z(2p_{xy})$ transitions of shallow donors in ZnO.[16] The $1s \rightarrow 2p_{xy}$ transition is the E mode and, therefore, should be ruled out since this assign-

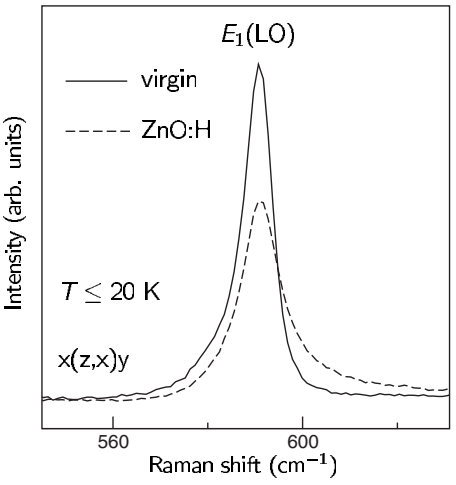

FIG. 3. Raman spectra obtained on a ZnO sample in the $x(z,x)y$ geometry at $T \leq 20$ K. Solid line—before hydrogenation. Dashed line—recorded directly after treatment in the H_2 gas at 725 °C.

ment contradicts the polarized Raman data presented in Fig. 2.

From theory, the splitting between the $2s$ and $2p_z$ states depends on the ionization energy of the donor, and is around 20 cm^{-1}.[16] In principle, both $2s$ and $2p_z$ states could be detected in Raman scattering.[33] The substantial linewidth [full width at half maximum (FWHM) ≈ 30 cm^{-1}], however, prevents us from a definitive assignment of the 330 cm^{-1} line. Later we will show that our data are more in favor of the $2p_z$ state.

In the following sections, we will give strong evidence that the 330 cm^{-1} electronic transition, the 3611 cm^{-1} (H-I) vibrational mode, and the donor ionization energy of 53 meV all belong to the H_{BC} donor in ZnO.

2. *Thermal stability of* H_{BC}

The thermal stability of the H_{BC} donor is studied by isochronal annealing. Figure 4 represents normalized intensities of the 330 cm^{-1} line as a function of the annealing temperature. The three panels in the figure show the results obtained on the ZnO samples treated in the H_2 (top), D_2 (mid), and H_2+D_2 (bottom) gas at 725 °C for 1 h. In addition, the normalized intensities of the local vibrational modes of the H-I (3611 cm^{-1}) and D-I (2668 cm^{-1}) defects are presented.

The temperature dependences of the 330 and 3611 cm^{-1} lines are almost identical. In the case of hydrogen, the signals remain constant up to 110 °C and anneal out at 190 °C. Note that this finding is consistent with the previous IR absorption studies on the 3611 cm^{-1} line.[22] The identical thermal behavior of the H-I defect and the 330 cm^{-1} line is a strong evidence that the two signals have the same origin.

The annealing data obtained from a ZnO sample treated with deuterium indicate a somewhat higher stability for D-I: the stretch mode at 2668 cm^{-1} and the 330 cm^{-1} line retain constant intensity up to 150 °C, and anneal out at about 230 °C.

The different thermal stabilities of H-I and D-I are an important result. The data presented in the top and the mid panels of Fig. 4, however, were obtained on different samples. To exclude the possibility of some secondary effects, not related to the nature of H-I, annealing experiments on a ZnO sample treated in a mixture of H_2 and D_2 were performed. The results are presented in the bottom panel of Fig. 4. Under these conditions D-I remains more stable as compared to H-I. What is also important, the intensity of the 330 cm^{-1} line follows neither of the other two curves but is positioned approximately in between. The finding gives additional support for the electronic nature of the 330 cm^{-1} line.

Summarizing the results, we propose that the different thermal stability of H-I (H_{BC}) and D-I (D_{BC}) comes from different diffusion rates of the two isotope species. A transition of H_{BC} into another configuration, i.e., H_{AB}, should be ruled out since, according to theory, bond-centered hydrogen aligned along the c axis is the ground state of isolated hydrogen in ZnO.[11,34] In addition, no local mode appearing at the expense of the 3611 cm^{-1} line is observed in the IR spectra.

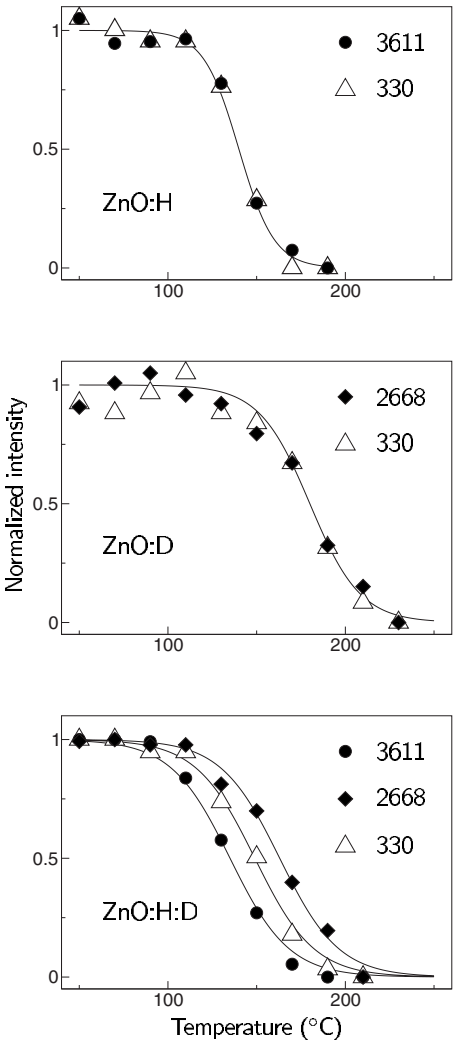

FIG. 4. Normalized intensities of the 330 cm^{-1} line and the local vibrational modes of the H-I (3611 cm^{-1}) and D-I (2668 cm^{-1}) defect as a function of annealing temperature. The hydrogenation was performed via thermal treatment at 725 °C in H_2 (top), D_2 (mid), and a mixture of H_2+D_2 (bottom) gases in the ratio 1:1. The solid lines are a guide to the eye.

In our model, H-I (H_{BC}) anneals out via diffusion and a subsequent trapping at some other defect. Provided H_{BC} is dominant, the formation of a dihydrogen complex, i.e., a hydrogen molecule, H_2, seems to be plausible.[3] Indirect indication to this possibility follows from the higher thermal stability of D-I in the ZnO sample treated in D_2 as compared to the mixture of H_2 and D_2 (see Fig. 4). Formation of the HD molecule is a natural explanation for this behavior in the framework of our model.

Hydrogen motion in ZnO was recently investigated by the stress-induced dichroism.[10,20,35] In particular, it was established that the activation energy of the hydrogen motion in copper-hydrogen complexes is thermally activated with an activation barrier for deuterium being somewhat higher than that of hydrogen. Such a behavior is known from other materials already. Usually, it is explained by the difference in the zero-point energy of the X-H and X-D species.[36] Here, X denotes the host atom.

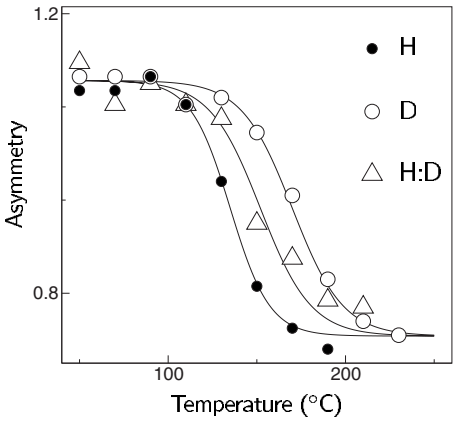

FIG. 5. Asymmetry of the E_1(LO) phonon line at 591 cm^{-1} in ZnO measured at $T \leq 20$ K in the $x(z,x)y$ geometry. The samples were treated in H_2, D_2, or H_2+D_2 at 725 °C. The solid lines are a guide to the eye.

In the case of the copper-dihydrogen complex (CuH_2) the onset of hydrogen motion around Cu atom occurs at 87 K, compared to 116 K for deuterium.[10] This difference in temperature corresponds to a difference in the activation energy of about 0.1 eV.

Our model is consistent with the previous assignment of H-I to bond-centered hydrogen.[5] Indeed, H_{BC} is a shallow donor in ZnO,[11] and therefore the electronic transition at 330 cm^{-1} and the H-I stretch mode should exhibit an identical annealing behavior. Moreover, we expect a direct correlation of the E_1(LO) phonon line shape with the H_{BC} concentration.

In order to describe quantitatively the influence of the annealing temperature on the line shape of the E_1(LO) phonon, we introduce the asymmetry $A=(\omega_+-\omega_0)/(\omega_0-\omega_-)$ of the line. Here, ω_0 is the frequency at maximum intensity, whereas ω_+ and ω_- are the frequencies obtained at half maximum on the high- and low-frequency sides of ω_0, respectively.

Figure 5 shows the asymmetry of the E_1(LO) phonon mode at 591 cm^{-1} obtained on the same set of ZnO samples as those presented in Fig. 4. The comparison of the figures suggests a very similar annealing behavior of the 330 cm^{-1} line and asymmetry of the E_1(LO) phonon mode.

This result is consistent with our suggestion that the change in the line form of the E_1(LO) phonon signal is due to the Fano resonance resulting from the continuum of the electronic states in the conduction band of shallow donors formed via hydrogenation. Moreover, the correlation between the stretch mode of H-I, electronic transition at 330 cm^{-1}, and the asymmetry of the E_1(LO) phonon suggests that the dominating donor is the bond-centered hydrogen.

If the 330 cm^{-1} line is the $1s \rightarrow 2p_z$ transition we can estimate the ionization energy (E_d) of H_{BC}. With the parameters presented in Ref. 16 we obtain $E_d \approx 53$ meV, which is very close to the ionization energy of the effective-mass shallow donor in ZnO at 50.15 meV.[16]

3. Concentration of H_{BC}

In polar semiconductors the Coulomb interaction between the infrared-active lattice vibrations and the free carriers leads to a coupling of the LO optical phonons and the plasmon vibrations.[32] The resulting phonon-plasmon modes show a distinct frequency shift compared to the uncoupled excitations. We use changes in the line shape to estimate the concentration of H_{BC}.

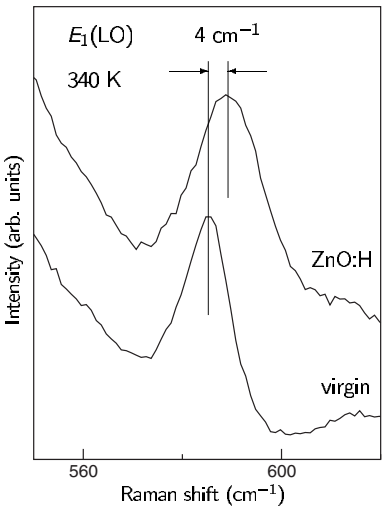

FIG. 6. Raman spectra of the E_1(LO) phonon measured at 340 K in the $x(z,-)y$ geometry on a virgin ZnO sample and the same sample after treatment in H_2 at 725 °C.

Figure 6 shows Raman spectra of the E_1(LO) phonon mode at a sample temperature of 340 K before and after hydrogenation. As expected, the hydrogenation results in a frequency shift $\Delta\omega$ and a broadening of the Raman line. From the data presented in the figure we obtain $\Delta\omega = 4$ cm^{-1}.

In the limit of small $\Delta\omega$, the frequency shift is a linear function of free-carrier concentration n (Ref. 37)

$$\Delta\omega \approx \frac{\omega_p^2}{2\omega_{LO}} \frac{\epsilon_0 - \epsilon_\infty}{\epsilon_0}. \quad (1)$$

Here, $\omega_p = \sqrt{4\pi e^2 n/\epsilon_\infty m^*}$ is the plasma frequency, $m^* = 0.27 m_0$ the effective mass of the electron, e the elementary charge, and $\epsilon_\infty = 4$ and $\epsilon_0 = 8$ are the high-frequency and the static dielectric constants, respectively.[38] Note that for the sake of simplicity we assume that ϵ_∞ and ϵ_0 are isotropic. The plasmon damping is also disregarded.

Substituting the value of $\Delta\omega = 4$ cm^{-1} into Eq. (1), we obtain at 340 K a concentration of free carriers of around 10^{17} cm^{-3}. This concentration corresponds directly to the amount of electrically active shallow donors.

In Fig. 7 the free-carrier concentration determined from $\Delta\omega$ is plotted against the sample temperature. The solid line is calculated for one shallow donor ionization energy.

The density of the states in the conduction band at RT was assumed to be $N_c = 4 \times 10^{18}$ cm^{-3}.[39] The best agreement with the experimental data is obtained for a donor ionization energy of $E_d = 52 \pm 2$ meV and the concentration of $N_d = (1.5 \pm 0.2) \times 10^{17}$ cm^{-3}. The value of E_d agrees quite well with the one obtained from the frequency of the electronic transition at 330 cm^{-1}.

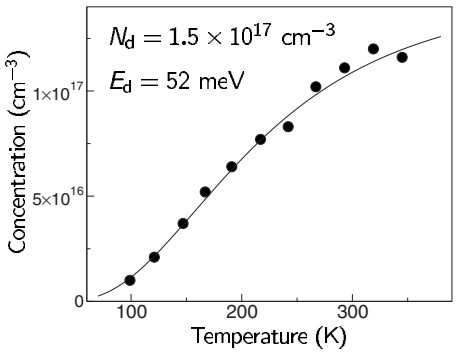

FIG. 7. Free carrier concentration in a ZnO sample obtained from the E_1(LO) phonon frequency as a function of temperature. Solid line—fit assuming that the main donor has an ionization energy of E_d=52 meV and concentration of 1.5×10^{17} cm^{-3}.

Note that our value of N_d is about a factor of 1.5 less than the one obtained from free-carrier absorption experiments.[22] In the referenced work, ZnO samples received a hydrogen treatment very similar to ours. Earlier studies of the phonon-plasmon coupling in ZnO have already established that the free-carrier concentration determined from the frequency shift of the E_1(LO) phonon is somewhat underestimated as compared to the one determined from the electrical measurements.[37] The difference decreases with increasing concentration. For the concentration of $N_d=1.5\times10^{17}$ cm^{-3} in our samples, the discrepancy is within 30%. Despite the differences in the donor concentration we find no change in the value of E_d if we scale up $n(T)$ by a factor of 1.3.

The passivation of compensating acceptors could also contribute to an E_1(LO) phonon shift. This situation is observed, for example, in hydrothermally grown ZnO where introduction of hydrogen results in formation of the neutral Li…H-O complex rather than H_{BC}.[8,40] In this case, however, the corresponding shallow donors give rise to $1s\rightarrow2s(2p_z)$ transitions with frequencies distinctly different from the 330 cm^{-1} line.[41] We rule out a pronounced acceptor passivation in our samples and attribute the phonon shift only to the generation of shallow H_{BC} donors.

B. IR absorption

1. Calibration of the 3611 cm^{-1} mode

Previously, the concentration of hydrogen defects was obtained qualitatively from the absorption of different stretch LVMs.[3,17] In IR absorption, the concentration of absorbing species is usually calculated from the intensity of the local mode and the corresponding effective charge e^*.[42] Our Raman data presented in the previous section give us the concentration of H_{BC} and allow directly a calibration of the stretch mode at 3611 cm^{-1}. For a concentration of $N_{3611}=N_d=1.5\times10^{17}$ cm^{-3} we determine the value of e^*. If α denotes the absorption coefficient of the local mode, the effective charge can be estimated from[43]

$$A \equiv \int \alpha(\sigma)d\sigma = \frac{\pi e^{*2} N_{3611}}{nc^2 \mu_{\text{O-H}}}, \tag{2}$$

where n is the refractive index, c the velocity of light, $\mu_{\text{O–H}}$ the reduced mass of the O-H bond, and $\sigma=\lambda^{-1}$ the wave number.

A value of $A=3.6$ cm^{-2} was determined for the sample from Fig. 7. We obtain $e^*=(0.28\pm0.03)e$ with an error due to the uncertainty in N_{3611}. For practical purpose Eq. (2) is rewritten to allow a direct determination of the H_{BC} concentration,

$$N_{3611} = (4.6 \pm 0.4) \times 10^{16} \text{ cm}^{-1} \int \alpha(\sigma)d\sigma. \tag{3}$$

Equal concentrations of absorbing species give according to Eq. (2) an absorption coefficient which is inversely proportional to the effective mass μ. We checked this dependence by treating a ZnO sample in D_2 gas. From the Raman shift on E_1(LO) and the position of the 330 cm^{-1} line, we established that the concentration of shallow donors and their ionization energy are equal in the H_2 and D_2 treated samples. In accordance with Eq. (2) the absorption coefficient measured on the 2668 cm^{-1} line of D-I dropped by a factor of 1.6, which is in reasonably good agreement with the expected ratio of $\mu_{\text{O-D}}/\mu_{\text{O-H}}=1.9$.

2. Shift of the 3611 cm^{-1} mode in an uniaxial stress field

The local vibrational mode of H_{BC} was predicted to shift upward in frequency by 4–5 cm^{-1}/GPa under hydrostatic compression.[44,45] In our study, we derive the hydrostatic shift from the splitting of the H_{BC} mode under uniaxial stress.

In linear approximation, the frequency of a nondegenerate LVM shifts with stress σ_{ik} as

$$\Delta\omega = \sum_{i,k} A_{ik}\sigma_{ik}. \tag{4}$$

For hydrostatic pressure $\sigma_{ik}=\sigma\delta_{ik}$ and Eq. (4) becomes

$$\Delta\omega = \sigma \,\text{Tr}(A). \tag{5}$$

Thus, the hydrostatic shift of LVM is given by the trace of A_{ik}. The trace of a second-ranked tensor does not depend on the coordinate system. Tr(A) can therefore be determined from the uniaxial stress experiments provided the stress pattern is known for three orthogonal directions.

Local vibrational modes of several hydrogen-related defects were recently studied under uniaxial stress and hydrostatic compression.[7,23,46] None of the defects investigated revealed the proposed hydrostatic shift of LVM upward in frequency. The influence of uniaxial stress parallel to the c axis on the 3611 cm^{-1} line was also investigated previously.[46] It was found that this mode does not shift with the stress ($A_{\parallel}=0$ cm^{-1}/GPa). No experiments for stress applied perpendicular to c were carried out and the hydrostatic shift could not be determined. In the present study we perform uniaxial stress experiments for $\boldsymbol{F}\parallel[10\bar{1}0]$. The results are presented in Fig. 8.

For $\boldsymbol{F}\parallel[10\bar{1}0]$, the 3611 cm^{-1} mode shifts upward in frequency with stress. The data in figure are fitted by $A_{\perp}=1$ cm^{-1}/GPa. For trigonal symmetry the hydrostatic pressure shift is given by $\text{Tr}(A)=A_{\parallel}+2A_{\perp}=2$ cm^{-1}/GPa. The factor of two stands for two orthogonal directions perpendicular to c. The result is roughly half the value of the theoretical prediction[44,45] but is in qualitative agreement with the identification of H_{BC} as the H-I center.

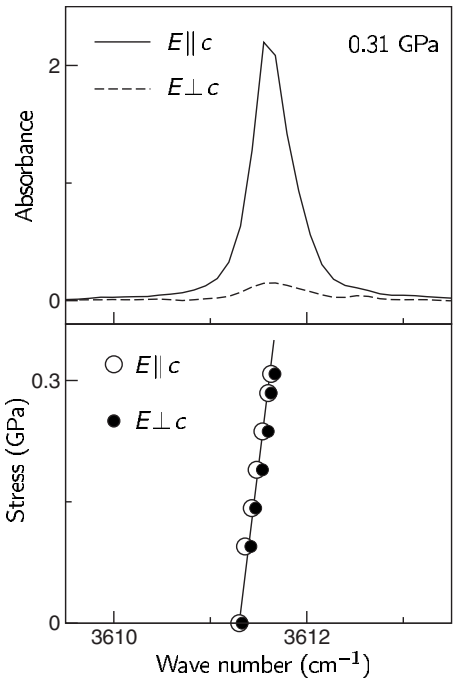

FIG. 8. IR absorption spectra and frequency shift of the 3611 cm^{-1} mode of the H-I defect obtained at $T \leq 10$ K under uniaxial stress $\boldsymbol{F} \| [10\bar{1}0]$. $\boldsymbol{k} \| [1\bar{2}10]$.

C. Photoluminescence

1. Identification of an excitonic recombination at H_{BC}

First, we consider the PL results obtained on the ZnO samples hydrogenated from plasma. Previously, it has been shown that this method results in the formation of H-I.[5] The plasma treatment generates a strongly nonuniform hydrogen profile with most of the hydrogen located at the sample surface. The laser only excites the surface-near regions and therefore the PL spectra are not disturbed by the low hydrogen bulk concentrations. The hydrogenation from plasma is performed at substantially lower temperatures in comparison with the thermal treatment in the H_2 gas. This results in much less surface damage and reduces the generation of nonradiative recombination centers.

Figure 9 shows the PL spectra of a ZnO sample taken at 4.2 K in the no-phonon region of excitons bound to shallow donors. The solid line in the figure is the spectrum recorded from the virgin sample, whereas the dashed line represents the spectrum taken after hydrogenation at 350 °C in a plasma.

The dominant signals in the virgin ZnO sample are those labeled D^+X, I_5, I_6, and I_9. The D^+X features are assigned to the excitons bound to ionized donors,[16] which indicates that some residual acceptors, most likely substitutional Li,[47] are present in the virgin material. The I_6 and I_9 lines are associated with excitons bound to the shallow donors due to substitutional Al and In, respectively.[16] The nature of the I_5 line remains unknown. Introduction of hydrogen changes the PL spectrum. The D^+X features disappear implying that hydrogen passivates the residual acceptors. What is more important, a new signal labeled H_{BC} at 3360.1 meV dominates the

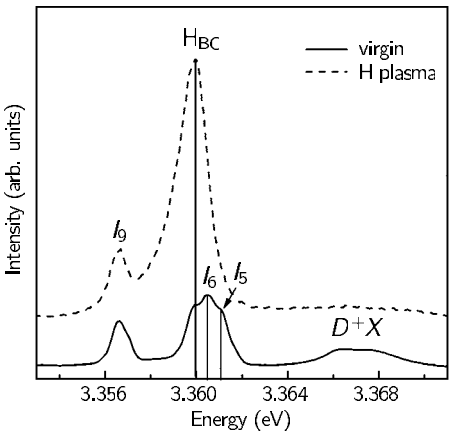

FIG. 9. Sections of PL spectra of a ZnO sample taken in the bound exciton region at 4.2 K. Solid line—virgin material. Dashed line—after hydrogenation in a dc plasma at 350 °C. The spectra are normalized to the I_9 line and are offset for clarity.

spectrum. Two features labeled I_{6a} (3360.4 meV) and I_7 (3360.0 meV) could, in principle, be associated with H_{BC}.[16] However, usually line positions in ZnO are strongly affected by sample conditions. A difference of around ±0.2 meV was reported.[16,25] Therefore, an identification of PL lines based solemnly on line positions is very speculative. A left-side shoulder at the I_6 line in the spectrum of the virgin ZnO sample indicates that the I_{6a}/I_7 lines are present already in the PL spectra *before* hydrogenation and, thus, cannot be assigned to hydrogen centers.

From our results reported in the previous sections, we know that our hydrogenated sample contains concentrations of the shallow hydrogen donor H_{BC} in the order of 10^{17} cm^{-3}. The energy of the corresponding excitonic no-phonon transition ($E_{H_{BC}}$) can be predicted on the basis of "Haynes rule."[16,25] From the donor energy of $E_d = 53$ meV obtained in Sec. III A, we determine a line position at $E_{H_{BC}} \approx 3360.0$ meV. The estimated energy for the exciton bound to the shallow donor due to H_{BC} is in remarkable agreement with the line position of the new PL at 3360.1 meV. Later on, we will give additional support for the identification of the PL line as due to H_{BC} donor. We will in the following label the PL line as H_{BC} instead of using the I_n nomenclature.

Figure 10 represents the two electron satellite (TES) sections of the same samples used in Fig. 9. A TES transition occurs when, in the exciton recombination process, the donor electron is excited from the ground state in a higher state. The energy difference between the bound exciton line and the TES line corresponds to the energy difference between the excited and the ground states of the donor. The strongest TES lines are excitations into the $2s$ and $2p$ states. Transitions to higher excited states were not reported in ZnO.

Figure 10 shows a strong signal at 3319.3 meV in the hydrogen plasma treated sample. This signal correlates with the 3360.1 meV line. The energy difference between the two signals 3360.1−3319.3=40.8 meV matches quite well the 330 cm^{-1}=40.9 meV line of H_{BC} from the Raman spectra.

Additional support for H_{BC} as the origin of the 3360.1 meV line comes from the thermal behavior of the PL line. The annealing data presented in Fig. 4 show a different ther-

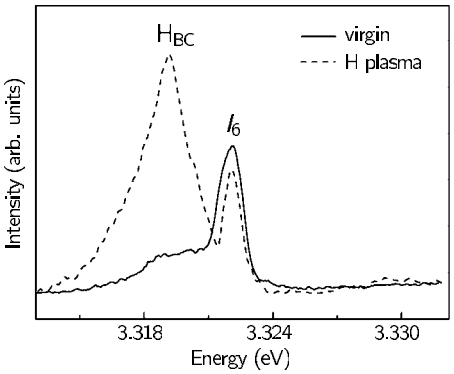

FIG. 10. Sections of the PL spectra of a ZnO sample taken in the TES region of excitons bound to neutral donors. $T=4.2$ K. Solid line—virgin material. Dashed line—after hydrogenation from a dc plasma at 350 °C. The spectra are normalized to the I_9 line.

mal stability for bond-centered hydrogen and deuterium. The PL data should also reveal this difference between the two isotopes.

Figure 11 shows the intensity of the 3360.1 meV line as a function of the annealing temperature. The filled circles and triangles stand for the results obtained on the samples treated with hydrogen and deuterium, respectively. As expected, the thermal stability of the 3360.1 meV line depends on the hydrogen isotope: the signal due to H_{BC} does not change up to 110 °C, whereas that of D_{BC} retains constant intensity up to 150 °C. This behavior agrees quite well with the thermal stability of H_{BC} (D_{BC}) obtained from the Raman data.

At higher annealing temperatures the intensity of the 3360.1 meV line increases again. This behavior seems to contradict the data presented in Fig. 4. We explain the growth of the 3360.1 meV line at higher temperatures by a local enhancement of the bond-centered hydrogen concentration. At elevated temperatures bond-centered hydrogen becomes mobile and diffuses from the bulk to the surface, thus increasing the concentration close to the surface.

2. I_4 donor

A no-phonon recombination of excitons bound to a hydrogen donor, the I_4 line, was reported at 3362.8 meV. The

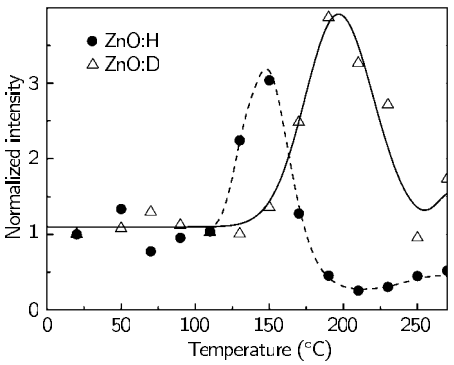

FIG. 11. Intensity of the 3360.1 meV line as a function of the annealing temperature. The samples were hydrogenated via thermal treatment in the H_2 (●) or D_2 (△) gas at 725 °C. The signals are normalized to the I_9 line. The solid lines in the figure are a guide to the eye.

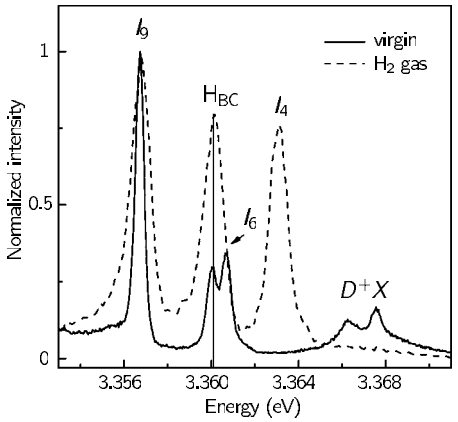

FIG. 12. PL spectra of a ZnO sample taken in the bound exciton region at 4.2 K. Solid line—virgin material. Dashed line—after treatment at 725 °C in the H_2 gas for 1 h. The spectra are normalized to the I_9 line.

ionization energy of the corresponding shallow donor I_4 is 47 meV.[16,25] Theory proposes two hydrogen donors in ZnO: bond-centered hydrogen, H_{BC}, and hydrogen trapped within the oxygen vacancy, H_O.[11,12] Our results strongly indicate that the latter donor is a reasonable model for I_4.

As shown in Fig. 9, the treatment of the samples in a hydrogen plasma at 350 °C gives rise only to H_{BC}. In contrast, samples treated in H_2 gas at higher temperatures exhibit the I_4 line. Results are presented in Fig. 12.

Two spectra are given in the figure: the one taken on a virgin ZnO sample (solid line) and the one obtained directly after thermal treatment in the H_2 gas at 725 °C for 1 h (dashed line). Only thermal treatment at high temperatures in H_2 gives rise to the I_4 line. The corresponding TES signal due to the $2p$ excitation, shifted by 33.2 meV from the main line at 3362.8 meV, was also detected.

We note a broadening of all PL lines in the H_2 gas annealed samples. Apparently, the high-temperature treatment damages the sample surface, and leads to defects and strain close to the surface. The plasma treatment at moderate 350 °C generates sharp PL lines, indicating a damage free introduction of hydrogen into the sample. In Fig. 12 the intensities of I_4 and H_{BC} are approximately equal. On the other hand, the $1s \rightarrow 2p$ excitation of the I_4 donors at 265 cm^{-1} (see Ref. 16) could not be detected in our Raman spectra from this sample (see Sec. III A).

3. H_{BC} versus I_4

A ZnO sample was treated in H_2 gas at 745 °C for 1 h. Subsequently, the sample was etched in orthophosphoric acid to generate a wedge (see Sec. II). The PL spectra were recorded at different heights of the sample, which corresponds to different depths below the original surface. Figure 13 plots the normalized PL intensities of H_{BC} and I_4 donors vs sample depth.

The profiling experiments were performed for several samples treated at temperatures from 695 to 765 °C. In all cases we found that the concentrations of I_4 and that of H_{BC} anticorrelate: the majority of the I_4 donors is located at the

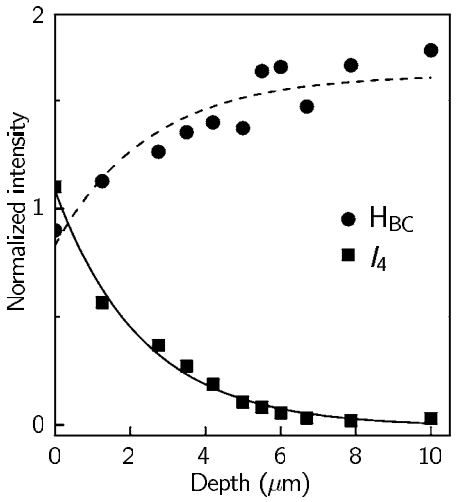

FIG. 13. Intensity profiles of the PL lines due to H_{BC} and I_4 taken at 4.2 K as a function of ZnO sample depth. The sample was treated in H_2 at 745 °C for 1 h. The intensities are normalized to I_9. The lines are fits to the data (see text).

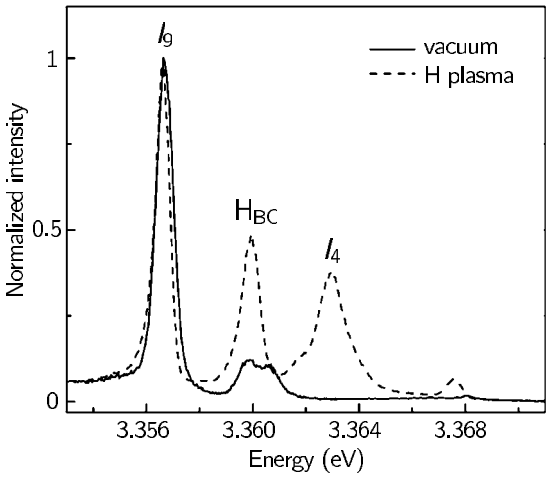

FIG. 14. PL spectra of a ZnO sample taken in the bound exciton region at 4.2 K. Solid line—after anneal in vacuum at 725 °C for 1 h. Dashed line—after subsequent hydrogenation from plasma at 350 °C. The spectra are normalized to the I_9 line.

sample surface and decreases exponentially with the sample depth, whereas the bond-centered hydrogen has a minimum concentration at the sample surface and a constant concentration in the bulk of the sample. The solid line in Fig. 13 corresponds to an exponential profile for $I_{I_4} \propto \exp(-\gamma x)$. The dashed line for the H_{BC} concentration assumes a complementary dependence $I_{H_{BC}} \propto A - \exp(-\gamma x)$. The penetration depth $\gamma^{-1}=2$ μm is the best fit to the data.

The inhomogeneous donor concentrations explain the missing Raman signal of the I_4 donor in the samples treated in H_2 gas. Our Raman measurements probe the bulk rather than the surface of the ZnO samples. The anticorrelation between H_{BC} and I_4 is an important result which implies that the formation of the I_4 donor occurs at the expense of the bond-centered hydrogen.

Annealing of ZnO in oxygen-poor ambient at elevated temperatures leads to a preferential loss of oxygen atoms. Close to the surface the excess of Zn leads to a nonstoichiometric composition.[48] The oxygen vacancy, V_O, is a low energy defect and should be easily formed at elevated temperatures in high concentrations.[49] This implies that the dominant defect resulting from the high-temperature treatment of ZnO in the oxygen-poor ambient is V_O.

In *n*-type ZnO the oxygen vacancy would be neutral and electrically inactive but the incorporation of hydrogen turns the vacancy into a shallow donor. The calculated binding energy of H_O with respect to H_{BC} and V_O was found to be 0.8 eV,[11] which is consistent with the thermal stability of I_4.

The absence of I_4 in the PL spectra after hydrogenation from plasma is explained by the low treatment temperature: there is no V_O available to form H_O at 350 °C. On the other hand, the formation of V_O is consistent with the concentration profiles of I_4 and H_{BC} shown in Fig. 13. The maximum excess of Zn is expected at the sample surface.

The identification of I_4 was supported by an experiment where first a virgin ZnO sample was annealed in *vacuum* at 725 °C for 1 h. The PL spectrum taken after this treatment is shown by the solid line in Fig. 14. Obviously, the vacuum anneal does not result in formation of any hydrogen donor but generates V_O in high concentrations. Subsequently, the ZnO sample was treated in a hydrogen plasma at 350 °C. Now the PL signals of I_4 and H_{BC} are detected in approximately equal intensities (dashed line of Fig. 14). A low-temperature plasma treatment without a preanneal at high temperatures gives no PL from I_4 (see Fig. 9).

Obviously, both hydrogen and the thermal treatment in the oxygen-poor ambient are necessary to form I_4. This result strongly supports our model of I_4 as a hydrogen bound to the oxygen vacancy, H_O.

The local mode of H_O is expected to be much lower in frequency compared to H_{BC} at 3611 cm^{-1}. Theory finds a value around 760 cm^{-1}.[12] It follows from here that IR absorption of LVM of H_O is almost impossible to detect because of the extremely strong absorption of ZnO in the corresponding spectroscopic region.[19] Raman scattering could be another means to detect the local mode. However, all H_O is located at the sample surface (see Fig. 13) and escapes detection in our Raman studies. An additional Raman investigation on ZnO samples with homogeneous concentration profiles of H_O is needed to detect the local vibrational mode of the defect.

D. Photoconductivity

The shallow hydrogen donors are studied by photothermal ionization spectroscopy (PTIS). Light excites an electron from the ground to one of the excited states of a donor and additional phonon absorption leads to an ionization of the donor.[50–52] PTIS is an extremely sensitive photoconductive technique. In Si and Ge a detection limit of shallow-impurity concentrations was calculated as low as 10^7 cm^{-3}.

The high sensitivity of PTIS is of special importance for ZnO where all $1s \rightarrow 2p$ transitions of the shallow donors are within or close to the Reststrahlen band between the lowest TO (380 cm^{-1}) and the highest LO (591 cm^{-1}) phonon

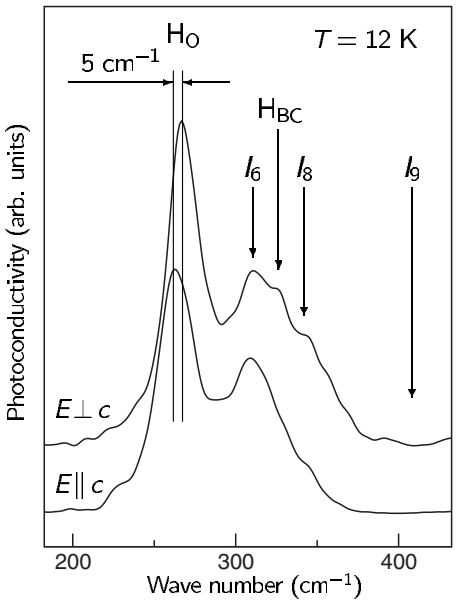

FIG. 15. Photoconductivity spectra taken at 12 K on a ZnO sample treated in the H_2 gas at 725 °C. $\boldsymbol{k}\|[10\bar{1}0]$

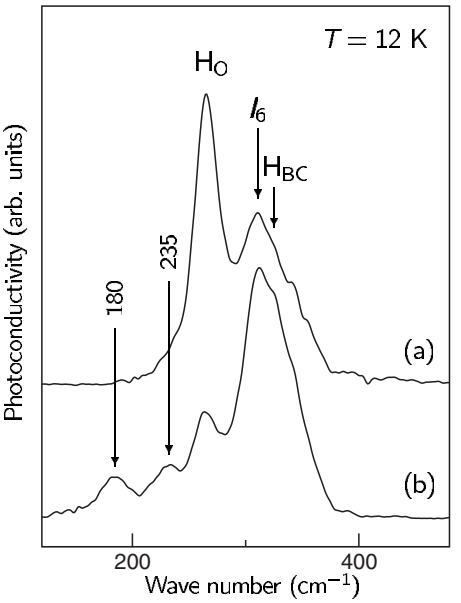

FIG. 16. Photoconductivity spectra taken at 12 K on a ZnO sample treated in the H_2 gas at 725 °C: (a) measured directly after the treatment, and (b) after removal of 5 μm from each surface of the sample. $\boldsymbol{k}\|[10\bar{1}0]$

modes. In this spectral range the reflectivity and/or absorption of the bulk ZnO are large,[53–56] thus making a direct absorption measurement on these transitions an extremely challenging task.

Recently, two photoconductivity studies of shallow donors in ZnO were reported. ZnO samples similar to the ones considered in this paper[19] and a virgin ZnO obtained from Eagle Picher[57] were investigated. It was shown that a number of photoconductivity lines appears after hydrogenation from a dc plasma, whereas the others are present in the virgin material already. In particular, the PTIS lines at 180, 240, and 268 cm^{-1} were tentatively associated with hydrogen shallow donors. The preliminary studies, however, did not lead to an identification of the shallow donors.

In this section we will present photoconductivity measurements on the ZnO samples, which were heat treated in H_2 gas. Figure 15 shows PTIS spectra obtained from a ZnO sample treated in H_2 at 725 °C. The measurements were performed with the polarizer aligned either parallel or perpendicular to the c axis. The line at about 265 cm^{-1} dominates the spectrum. The exact frequency of this transition depends on the polarizer orientation: 262 and 267 cm^{-1} for $\boldsymbol{E}\|\boldsymbol{c}$ and $\boldsymbol{E}\perp\boldsymbol{c}$, respectively. This frequency difference corresponds quite well to the splitting between the $2p_z$ and $2p_{xy}$ states of a shallow donor in ZnO.[16]

Moreover, the 265 cm^{-1} line matches exactly the energy of the $1s\rightarrow 2p$ transition obtained on the I_4 donor from PL studies.[16,25] The donor excitation confirms the identity of the I_4 donor with H_O. The arrows in Fig. 15 indicate the expected frequencies of the $1s\rightarrow 2p$ transitions of the other shallow donors seen in the PL spectra.

No signal from I_9 or the direct transitions from the donor ground state to the conduction band are detected due to the strong absorption in the Reststrahlen band. The estimated frequencies of the $1s\rightarrow 3p$ (325 cm^{-1}) and $1s\rightarrow 4p$ (345 cm^{-1}) transitions of the H_O donor coincide with the $1s\rightarrow 2p$ transitions originating from the H_{BC} and I_8 donors, respectively.[16] Therefore, we cannot rule out the possibility that part of the H_{BC} and I_8 signals seen in Fig. 15 originates from the $3p$ and $4p$ states of the H_O donor. Due to the considerable line broadening a more detailed analysis of the PTIS lines is not possible at present.

The 310 cm^{-1} line labeled I_6 was identified as the $1s\rightarrow 2p$ transition of the shallow donor Al. In Al doped ZnO samples the 310 cm^{-1} line dominates the spectra.[41] The line splits into two signals positioned at 307 and 312 cm^{-1} if the polarizer is aligned parallel and perpendicular to c, respectively. This behavior is consistent with the splitting between the p_z and p_{xy} states of a shallow donor in ZnO.[16]

In Fig. 16 two spectra from a ZnO sample treated in H_2 gas at 725 °C are given. Spectrum (a) belongs to the original sample, whereas (b) is measured after removing of 5 μm from the sample surface. The intensity of the H_O signal drops in spectrum (b), and two new lines at 180 and 235 cm^{-1} appear.

The change in the PTIS spectrum of the polished sample occurs in accordance with the PL results presented in Sec. III C. With sample depth the intensity of the H_O line becomes weaker than that of H_{BC}. Thus, photoconductivity measurements are consistent with depth profile of H_O obtained from PL.

The 265 cm^{-1} line dominates the PTIS spectra even though the H_O donors are located only within 5 μm of the sample surface. Such a high surface sensitivity makes PTIS a favorable technique to study ZnO thin films.

IV. DISCUSSION

Bond-centered hydrogen is a shallow donor in ZnO. We identified signals due to H_{BC} in Raman scattering, IR absorp-

tion, photoluminescence, and photoconductivity. This allowed us to determine the ionization energy of H_{BC} and investigate its thermal stability. From comparison of our experimental data against first-principles calculations microscopic structure of the defect was deduced: hydrogen primarily bound to an oxygen atom with the O-H bond aligned parallel to the *c* axis. The stretch mode of the O-H bond was shown to have a frequency of 3611 cm^{-1}.

Literature data seem to contradict our identification of H_{BC}. Previously, the local mode of H-I at 3611 cm^{-1} was associated with two electronic transitions at 1430 and 1480 cm^{-1}. From the frequency of these modes, a deep donor energy of around 200 meV was estimated.[19] Based on the connection of the H-I local mode with a deep donor, no correlation with the shallow donor H_{BC} was made.

A more careful analysis reconciles our interpretation of H_{BC}. Experiments have shown that H_{BC} is the dominant donor in our ZnO samples, which determines the position of the Fermi level. On the other hand, the Fermi-level position fixes the charge state of the defects. The LVM frequency of defects depends on the charge state. Therefore, a shift in Fermi level, e.g., by hydrogenation, will lead to a change in the intensity of the local mode. In the annealing experiments reported in Ref. 19 the intensity of the local modes was wrongly interpreted as the total defect concentration instead of the concentration of one charge state of the defect.

Based on the strong identification of the shallow donor H_{BC}, we suggest that the similar annealing behavior of the 1430, 1480, and 3611 cm^{-1} absorption lines is accidental, and the electronic transitions at 1430 and 1480 cm^{-1} are not related to H_{BC}.

Another correlation between the intensity of the 3611 cm^{-1} line and a line at 3326 cm^{-1} was detected.[22] Because the structure of the two defects is different (H_{BC} vs possibly $V_{Zn}H^{-}$), a direct association with the Fermi-level shift with hydrogenation was proposed.[20]

The 330 cm^{-1} Raman line of the H_{BC} shallow donor assigned to the $1s \rightarrow 2s(2p_z)$ transition should be difficult to observe according to theoretical consideration.[32] An exception could be expected, however, near resonance. For example, the $1s \rightarrow 2s(2p_z)$ transitions due to Cl donor in CdS were detected using the 488 nm line of the argon laser, which is close to the band gap of CdS.[33] Such a resonance is not possible in our study since the 532 nm line does not match the band gap of ZnO.

An investigation of the band structure of ZnO reveals another possible resonance.[38] The energy difference between the minimum of the conduction band and the next energy level at the Γ point of the Brillouin zone (Γ_3) is 2.25 eV. This value plus the ionization energy of an ideal shallow donor in ZnO gives 2.3 eV. This energy coincides with the 2.33 eV energy quantum of the 532 nm line. A strong intensity of the $1s \rightarrow 2s(2p)$ Raman transitions of shallow donors in ZnO is, therefore, possible by selecting the proper excitation energy.

The stability of isolated hydrogen (H_{BC}) is unexpected. Theory calculates a diffusion barrier of around 0.5 eV.[24] Under these conditions bond-centered hydrogen should be mobile at room temperature and high concentrations of H_{BC} would not be possible. Our experiments suggest that, however, the apparent stability of H_{BC} is due to the interaction with other defects.

Directly after hydrogenation the dominant defect in our ZnO samples is H_{BC}. Therefore, formation of hydrogen molecules, H_2, in the course of sample annealing can account for the apparent stability of isolated hydrogen.

As a shallow donor, bond-centered hydrogen is ionized and, therefore, positively charged at RT. The Coulomb repulsion between two neighboring H_{BC}^{+} slows down the formation rate of H_2 and explains the relative stability of bond-centered hydrogen in our samples.

Additional support for H_2 as a sink for H_{BC} comes from annealing data presented in Fig. 4. As pointed out already, the D-I signal is somewhat more stable in the sample treated in D_2 gas as compared to the mixture of H_2 and D_2. The diffusion of H_{BC} and D_{BC}, and the formation of the HD molecule explains this peculiarity.

Hydrogen molecule is expected to be invisible in IR absorption but could be detected in Raman scattering. First-principles calculation find that interstitial H_2 in ZnO is a free rotator with a stretch mode frequency of 4032 cm^{-1}.[34] We studied the corresponding spectroscopic region in the course of the annealing process of H_{BC}. No signal appeared in the Raman spectra at the expense of the 3611 cm^{-1} mode. We take this as an indication that the detection limit of our setup has to be enhanced in order to observe H_2.

Our identification of H_O is somewhat less profound in comparison with H_{BC}. This assignment is mainly based on the anticorrelation between the concentration profiles of these donors determined from the PL data presented in Sec. III C. Previous photoluminescence studies established that the shallow donor giving rise to the I_4 line is stable up to 500 °C.[16,25] This agrees with theoretical calculations presented in Ref. 12 and favors our assignment of the I_4 line to H_O.

Direct insight into the microscopic structure of H_O could be obtained from local mode frequency of this defect. Theory reports the value around 760 cm^{-1}.[12] Direct IR absorption studies in this region are, however, hardly possible.[19] A separate investigation of the local modes due to H_O by other means is needed to get insight into the chemistry of this defect.

Finally, we want to comment on the PTIS signals at 180 and 235 cm^{-1} (see Fig. 16). These lines appear after hydrogenation and were previously associated with hydrogen.[19] Assuming that these are $1s \rightarrow 2p$ transitions we obtain that the ionization energies of the corresponding shallow donors are 35 and 42 meV, respectively. A hydrogen donor with the ionization energy of 35 meV was also reported.[15] These findings indicate that H_{BC} and H_O are not the only hydrogen donors in ZnO, and further investigations are needed to deepen our knowledge of hydrogen behavior in this material.

V. CONCLUSIONS

Hydrogen donors in ZnO are studied by Raman scattering, IR absorption, photoluminescence, and photoconductivity. Two shallow donors are identified: bond-centered hydrogen, H_{BC}, and hydrogen bound within the oxygen vacancy, H_O.

H_{BC} is the dominant donor and appears directly after hydrogenation of vapor phase grown ZnO. The decay of an

exciton bound to H_{BC} results in the photoluminescence line at 3360.1 ± 0.2 meV. The internal $1s \rightarrow 2p$ transition of H_{BC} is detected at 330 cm^{-1} in the Raman scattering and photoconductivity spectra. The local vibrational mode of the O-H bond comprising the bond-centered hydrogen has a frequency of 3611 cm^{-1} (H-I) and an effective charge of $(0.28 \pm 0.03)e$. The concentration of H_{BC} was determined from the frequency shift of the $E_1(LO)$ phonon-plasmon mode at 591 cm^{-1}. The ionization energy of H_{BC} at 53 meV was established from the temperature dependence of the free-carrier concentration. Bond-centered hydrogen was found to be unstable against annealing at 190 °C. The stability is, however, determined by the diffusion process and the trapping by other defects. There is evidence that H_{BC} captures another H_{BC} and forms hydrogen molecules.

The H_O donor was shown to have an ionization energy of 47 meV. In photoluminescence, an excitonic recombination of the H_O donor results in the well-known I_4 line at 3362.8 meV. A $1s \rightarrow 2p_z(2p_{xy})$ electronic transition at 265 cm^{-1} of H_O is detected in the photoconductivity spectra. The donor is created by an anneal in oxygen-poor ambient with subsequent or simultaneous incorporation of hydrogen. The formation occurs via trapping H_{BC} at the vacancies left by the out-diffusing oxygen.

ACKNOWLEDGMENTS

The authors are indebted to R. Helbig for providing us with the ZnO samples. F. Börrnert is acknowledged for helping with the uniaxial stress measurements.

*edward.lavrov@physik.tu-dresden.de

[1] E. Mollwo, Z. Phys. **138**, 478 (1954).
[2] D. G. Thomas and J. J. Lander, J. Chem. Phys. **25**, 1136 (1956).
[3] G. A. Shi, M. Saboktakin, M. Stavola, and S. J. Pearton, Appl. Phys. Lett. **85**, 5601 (2004).
[4] F. G. Gärtner and E. Mollwo, Phys. Status Solidi B **89**, 381 (1978).
[5] E. V. Lavrov, J. Weber, F. Börrnert, C. G. Van de Walle, and R. Helbig, Phys. Rev. B **66**, 165205 (2002).
[6] L. E. Halliburton, L. Wang, L. Bai, N. Y. Garces, N. C. Giles, M. J. Callahan, and B. Wang, J. Appl. Phys. **96**, 7168 (2004).
[7] E. V. Lavrov and J. Weber, Phys. Status Solidi B **243**, 2657 (2006).
[8] G. A. Shi, M. Stavola, and W. B. Fowler, Phys. Rev. B **73**, 081201(R) (2006).
[9] S. J. Jokela and M. D. McCluskey, Phys. Rev. B **76**, 193201 (2007).
[10] E. V. Lavrov, J. Weber, and F. Börrnert, Phys. Rev. B **77**, 155209 (2008).
[11] C. G. Van de Walle, Phys. Rev. Lett. **85**, 1012 (2000).
[12] A. Janotti and C. G. Van de Walle, Nature Mater. **6**, 44 (2007).
[13] S. F. J. Cox, E. A. Davis, S. P. Cottrell, P. J. C. King, J. S. Lord, J. M. Gil, H. V. Alberto, R. C. Vilão, J. Piroto Duarte, N. Ayres de Campos, A. Weidinger, R. L. Lichti, and S. J. C. Irvine, Phys. Rev. Lett. **86**, 2601 (2001).
[14] K. Shimomura, K. Nishiyama, and R. Kadono, Phys. Rev. Lett. **89**, 255505 (2002).
[15] D. M. Hofmann, A. Hofstaetter, F. Leiter, H. Zhou, F. Henecker, B. K. Meyer, S. B. Orlinskii, J. Schmidt, and P. G. Baranov, Phys. Rev. Lett. **88**, 045504 (2002).
[16] B. K. Meyer, H. Alves, D. M. Hofmann, W. Kriegseis, D. Forster, F. Bertram, J. Christen, A. Hoffmann, M. Straßburg, M. Dworzak, U. Haboeck, and A. V. Rodina, Phys. Status Solidi B **241**, 231 (2004).
[17] M. D. McCluskey, S. J. Jokela, K. K. Zhuravlev, P. J. Simpson, and K. G. Lynn, Appl. Phys. Lett. **81**, 3807 (2002).
[18] C. H. Seager and S. M. Myers, J. Appl. Phys. **94**, 2888 (2003).
[19] E. V. Lavrov, F. Börrnert, and J. Weber, Phys. Rev. B **72**, 085212 (2005).
[20] E. V. Lavrov, F. Börrnert, and J. Weber, Physica B **401-402**, 366 (2007).
[21] X.-B. Li, S. Limpijumnong, W. Q. Tian, H. B. Sun, and S. B. Zhang, Phys. Rev. B **78**, 113203 (2008).
[22] G. A. Shi, M. Stavola, S. J. Pearton, M. Thieme, E. V. Lavrov, and J. Weber, Phys. Rev. B **72**, 195211 (2005).
[23] S. J. Jokela and M. D. McCluskey, Phys. Rev. B **72**, 113201 (2005).
[24] M. G. Wardle, J. P. Goss, and P. R. Briddon, Phys. Rev. Lett. **96**, 205504 (2006).
[25] A. Schildknecht, R. Sauer, and K. Thonke, Physica B **340-342**, 205 (2003).
[26] G. Müller and R. Helbig, J. Phys. Chem. Solids **32**, 1971 (1971).
[27] R. Helbig, J. Cryst. Growth **15**, 25 (1972).
[28] E. V. Lavrov and J. Weber, Phys. Rev. B **73**, 035208 (2006).
[29] *CRC Handbook of Chemistry and Physics*, edited by D. R. Lide (CRC, New York, 2001).
[30] C. A. Arguello, D. L. Rousseau, and S. P. S. Porto, Phys. Rev. **181**, 1351 (1969).
[31] U. Fano, Phys. Rev. **124**, 1866 (1961).
[32] M. V. Klein, in *Light Scattering in Solids I*, edited by M. Cardona (Springer-Verlag, Berlin, 1983), pp. 147–204.
[33] C. H. Henry and K. Nassau, Phys. Rev. B **2**, 997 (1970).
[34] M. G. Wardle, J. P. Goss, and P. R. Briddon, Phys. Rev. B **72**, 155108 (2005).
[35] F. Börrnert, E. V. Lavrov, and J. Weber, Phys. Rev. B **75**, 205202 (2007).
[36] Y. M. Cheng and M. Stavola, Phys. Rev. Lett. **73**, 3419 (1994).
[37] B. H. Bairamov, A. Heinrich, G. Irmer, V. V. Toporov, and E. Ziegler, Phys. Status Solidi B **119**, 227 (1983).
[38] O. Madelung, *Semiconductors: Data Handbook* (Springer-Verlag, New York, 2004).
[39] C. Klingshirn, Phys. Status Solidi B **244**, 3027 (2007).
[40] E. V. Lavrov, F. Börrnert, and J. Weber, Phys. Rev. B **71**, 035205 (2005).
[41] E. V. Lavrov, F. Herklotz, and J. Weber (unpublished).
[42] R. C. Newman, in *Semiconductors and Semimetals*, edited by E. R. Weber (Academic, Boston, 1993), Vol. 38, p. 117.
[43] E. Bright Wilson, Jr., J. C. Decius, and C. Paul, *Cross, Molecular Vibrations* (Dover, New York, 1980).
[44] S. Limpijumnong and S. B. Zhang, Appl. Phys. Lett. **86**, 151910

(2005).
[45] M. G. Wardle, J. P. Goss, and P. R. Briddon, Appl. Phys. Lett. **88**, 261906 (2006).
[46] E. V. Lavrov and J. Weber, Phys. Rev. B **73**, 035208 (2006).
[47] B. K. Meyer, private communication.
[48] H. E. Brown, *Zinc Oxide: Properties and Applications* (International Lead Zinc Research Organization, New York, 1976).
[49] A. F. Kohan, G. Ceder, D. Morgan, and Chris G. Van de Walle, Phys. Rev. B **61**, 15019 (2000).
[50] Sh. M. Kogan and T. M. Lifshits, Phys. Status Solidi A **39**, 11 (1977).
[51] T. M. Lifshits, Instrum. Exp. Tech. **36**, 1 (1993).
[52] S. M. Myers, M. I. Baskes, H. K. Birnbaum, J. W. Corbett, G. G. DeLeo, S. K. Estreicher, E. E. Haller, P. Jena, N. M. Johnson, R. Kirchheim, S. J. Pearton, and M. J. Stavola, Rev. Mod. Phys. **64**, 559 (1992).
[53] R. J. Collins and D. A. Kleinman, J. Phys. Chem. Solids **11**, 190 (1959).
[54] G. Heiland and H. Lüth, Solid State Commun. **5**, 199 (1967).
[55] S. Perkowitz, R. K. Murty-Gutta, and A. K. Garrision, Solid State Commun. **9**, 2251 (1971).
[56] H. Finkenrath, K. Krug, and N. Uhle, Phys. Status Solidi B **78**, K27 (1976).
[57] U. Röder, D. Klarer, R. Sauer, and K. Thonke, *Proceedings of the 27th International Conference on the Physics of Semiconductors*, Flagstaff, AZ 2004, AIP Conf. Proc. No. 772, (AIP, New York, 2005), p. 179.